J Fluoresc (2009) 19:1073–1082
DOI 10.1007/s10895-009-0507-6

ORIGINAL PAPER

Synthesis, Crystal Structure, DNA-binding Properties and Cytotoxic Activity of the Copper (II) Complex Involving Xanthone

Rui Shen · Peng Wang · Ning Tang

Received: 2 March 2009 / Accepted: 5 June 2009 / Published online: 4 July 2009

Abstract 1, 8-(3, 6, 9-Trioxaundecane-1, 11-diyldioxy) xanthone (**L**), and its new Cu (II) complex $[Cu{\cdot}\mathbf{L}{\cdot}(CH_3CN)_2](ClO_4)_2$ have been synthesized and characterized by ^1H NMR, electrospray mass spectra (ESI-MS), elemental analyses, infrared spectra (IR) and X-ray single crystal diffraction. The crystal structure of complex shows that Cu (II) ion is encapsulated within the macrocycle of **L**. The geometry around copper is a distorted square bipyramid with two acetonitrile molecules at axial position, and four macrocyclic oxygens including the carbonyl oxygen on the equatorial positions. The interaction of Cu (II) complex with calf thymus DNA (ct DNA) has been investigated by spectrophotometric titrations, ethidium bromide (EB) displacement experiments, circular dichroism (CD) spectra and viscosity measurements. Rresults indicate that Cu (II) complex can intercalate into the DNA base pairs by the plane of xanthone ring. Furthermore, the Cu (II) complex was tested against tumor cell lines including ECA109, SGC7901and GLC-82 by MTT (microculture tetrazolium) method. The studies of DNA-binding agree with the effects on the inhibition of tumor cells in vitro.

Keywords Cu (II) complex · Xanthone · DNA-binding · Cytotoxicity

R. Shen (✉) · P. Wang
College of Pharmacy, Nankai University,
Tianjin 300071, People's Republic of China
e-mail: shenr05@lzu.cn

N. Tang
College of Chemistry and Chemical Engineering,
Lanzhou University,
Lanzhou 730000, People's Republic of China

Introduction

Binding studies of small molecules with deoxyribonucleic acid (DNA) on a molecular level become important for regulation of gene expression. A more complete understanding of how to target DNA sites with specificity will lead not only to novel chemotherapeutics but also to a greatly expanded ability for chemists to probe DNA and to develop highly sensitive diagnostic agents [1–6]. Transition-metal complexes are being used at the forefront of many of these efforts. These complexes can interact noncovalently with DNA by intercalation when the ligand contains planar ring systems, groove binding for large molecules, or external electrostatic binding for cations. The binding modes are dependent on the sizes and stereochemical properties of the complexes [7–11]. So stable, inert, and water-soluble complexes containing spectroscopically active metal centers are widely exploited for serving as probes for nucleic acid structure and showing nuclease property.

The numerous biological experiments have demonstrated that DNA is the primary intracellular target of anticancer drugs due to the interaction between small molecules and DNA, which cause DNA damage in cancer cells, inhibiting the division of cancer cells and resulting in cell death [12, 13]. Of those studies, interactions between metallic anticancer reagents and DNA are also very important in understanding the mechanisms of their anticancer activities [14–17]. These investigations are the basis of designing new and more efficient anticancer drugs.

Based on these considerations we have selected xanthone compounds which have a large variety of biological and pharmacological activities [18–21] and improved the hydrophilic property by simple chemical modification. Simultaneously, we have synthesized a novel Cu (II) complex involving xanthone (Fig. 1), utilizing the metal-

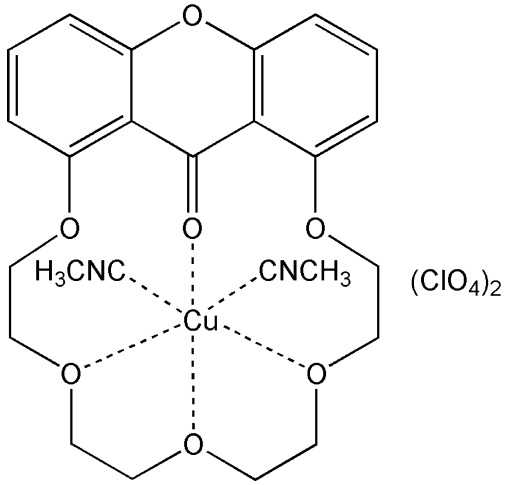

Fig. 1 The scheme of Cu (II) complex

ligand coordinative interaction and the special physiological activity of Cu^{2+} in vivo to vary the planarity of xanthone structure and increase the affinities of xanthone to DNA. Subsequently, we have investigated the mode of binding of the xanthone-Cu complex to DNA and its effect on the growth of three human cancer cell lines, ECA109 (esophagus squamous cancer), SGC7901 (stomach cancer) and GLC-82 (lung cancer) in vitro. Results of these experiments are expected to provide evidence for the nature of the binding of the xanthone-Cu complex to DNA and offer an impetus for designing newer DNA structure probes and DNA directed therapeutic agents.

Experimental

Materials

1, 8-(3, 6, 9-Trioxaundecane-1, 11-diyldioxy)xanthone (**L**) was prepared according to the procedure of Mills and Mooney with some improvement [22]. Copper (II)perchlorate hexahydrate was prepared according to the literature [23], other chemicals were reagent grade and were used without further purification. Calf thymus DNA (ct DNA) and ethidium bromide (EB) were obtained from Sigma Chemical Co.

Measurements

Elemental analyses were conducted using an Elementar Vario EL elemental analyzer, infrared spectra (IR) (4,000–400 cm^{-1}) were performed on a satellite FTIR spectrometer (Thermo Mattson) with KBr as discs, mass spectra (MS) were performed on a VG ZAB-HS instrument, electrospray mass spectra (ESI-MS) were obtained from a Finngan MAT LCQ instrument and ^{1}H NMR spectra were recorded using a Varian Mercury Plus 400 spectrometer. The UV-Vis absorption spectra were recorded using a Varian Cary 100 spectrophotometer, the fluorescence emission spectra were recorded using a Hitachi F-4500 spectrofluorophotometer and the circular dichroic (CD) spectra were recorded on a Olos RSM 1000 spectropolarimeter, respectively.

All the measurements involving the interaction of Cu (II) complex with ct DNA were carried out in doubly distilled water buffer containing 5 mM Tris and 50 mM NaCl, and adjusted to pH7.1 with hydrochloric acid. UV-Vis spectrometer was employed to check a solution of ct DNA purity (A_{260}: A_{280}>1.80) and concentration (ε=6,600 M^{-1} cm^{-1} at 260 nm) in the buffer [24, 25]. The Cu (II) complex was first dissolved in a minimum amount of ethanol (0.05 % of the final volume), and then diluted with Tris-HCl buffer (5 mM Tris-HCl, 50 mM NaCl, pH7.1) at concentration 5 μM.

Preparation of 1, 8-(3, 6, 9-Trioxaundecane-1, 11-diyldioxy)xanthone (**L**) [22]

1, 8-Dihydroxyxanthone (500 mg, 2.2 mmol) was dissolved in dry DMF (170 mL) in a three-necked flask with stirring, and anhydrous potassium carbonate (1.0 g) was added under N_2. 1, 11-dibromo-3, 6, 9-trioxaundecane (1.4 g, 4.4 mmol) was added via a syringe and the mixture refluxed for 14 h. Most of the DMF was evaporated under reduced pressure. The resulting mixture was diluted with water (30 mL), extracted several times with chloroform and the chloroform extracts evaporated. The residue was purified by column chromatography (SiO_2, $CHCl_3$-EtOH), and then recrystallized from dry toluene afforded **L** as off-white crystals (385 mg, 45.3%); mp.189–190°C; MS: 387.1 [M+1], 386.1[M]; ^{1}H NMR (400 MHz, $CDCl_3$, 25°C): δ 7.50–7.46 (t, 2 H, Ar-H), 6.97–6.95 (d, 2 H, Ar-H), 6.70–6.68 (d, 2 H, Ar-H), 4.23–4.20 (m, 4 H, O-CH_2), 4.02–3.97 (m, 8 H, O-CH_2-CH_2-O), 3.84–3.91 (m, 4 H, O-CH_2). IR (KBr): ν (C=O) 1,666.0, ν (C=C) 1,473.0, ν (C-O-C) 1,237.7, ν (Ar-O) 1,087.9, ν (Ar-H) 766.9 cm^{-1}.

Preparation of Cu (II) complex

L (77.2 mg, 0.2 mmol) was dissolved in 8 mL of acetonitrile. Copper (II) perchlorate hexahydrate (74.1 mg, 0.2 mmol) was dissolved in 2 mL of acetonitrile and added dropwise to the above solution. The mixture was stirred for 2 h and the solvent was evaporated under reduced pressure. The residue was redissolved in 5 mL of acetonitrile and layered with diethyl ether. Fine crimson block crystals were obtained. Yield: 116.9 mg (80%). ESI-MS [CH_3OH, m/z]: $[M\text{-}ClO_4]^+$ 550.1, $[M\text{-}2ClO_4]^{2+}$ 224.6. Elemental Anal. Calcd for $C_{25}H_{28}CuCl_2N_2O_{15}$: C, 41.08; H, 3.86; N,

3.83 %. Found: C, 39.95; H, 3.78; N, 3.92 %. IR (KBr): ν (C=O) 1,641.3, ν (C=C) 1,476.3, ν (C-O-C) 1,238.8, ν (Ar-O) 1,086.6, ν (Ar-H) 770.6, ν (M-O) 471.8 cm^{-1}.

X-ray crystallographic studies

Crystal of Cu (II) complex grown by vapor diffusion of acetonitrile / ether, was mounted on a Bruker SMART APEXII CCD diffractometer for data collection at 293(2) K using Mo Kα radiation. Final cell constants were calculated from the *xyz* centroids of typically more than 4,000 reflections from the data collection after integration. Structure was solved by direct methods using SHELXS-97 and refined using SHELXL-97. One perchlorate for the structure of complex was modeled as disordered over two positions (50:50). Table 1 lists additional crystal and refinement information.

Solution chemistry and stability studies

The absorption spectra in the UV-vis region were recorded at 25°C. The Cu (II) complex was first dissolved in a minimum amount of ethanol (0.05 % of the final volume), and then diluted with Tris-HCl buffer. The stability studies were carried out by monitoring the electronic spectra of the resulting mixtures over 72 h.

DNA interactions

Absorption and fluorescence titration experiments were performed by fixing the Cu (II) complex concentration as constant at 5 μM while varying the concentration of ct DNA. The competitive binding experiment was carried out by maintaining the EB and ct DNA concentration at 2 μM and 30 μM, respectively, while increasing the concentration of Cu (II) complex. Fitting was completed using an Origin 6.0 spreadsheet, where values of the binding constants K were calculated.

The circular dichroic spectra of DNA were scanned in the range of 200–350 nm at 25.0°C. The optical chamber of the CD spectrometer was deoxygenated with dry nitrogen before use and kept in a nitrogen atmosphere during experiments. Scans were accumulated and automatically averaged.The spectrum was generated which represented the average of three scans from which the buffer background had been subtracted. Ct DNA used were

Table 1 Crystal data and structure refinement for complex

	$[Cu{\cdot}\mathbf{L}{\cdot}(CH_3CN)_2](ClO_4)_2$
Empirical formula	$C_{25}H_{28}Cl_2N_2CuO_{15}$
Formula weight	730.93
Temperature	293(2)K
Diffractometer	Bruker CCD
Crystal system	orthorhombic
Space group	Pbca
a ,Å	20.6328(11)
b ,Å	14.1068(8)
c, Å	20.9568(11)
α,°	90.00
β,°	90.00
γ,°	90.00
V, $Å^3$	6,099.7(6)
Z	8
Density (calcd) $g{\cdot}cm^{-3}$	1.592
Absorb.coeff.mm^{-1}	0.966
F (000)	3,000
θ range	2.45–22.89
Iindex ranges	$-27 \le h \le 22$; $-18 \le k \le 18$; $-27 \le l \le 19$
Reflections collected/unique	35,413/7,398 [R(int)=0.0558]
Reflections observed	4,179
Date/restrains/parameters	7,398/0/447
GOF	1.017
Final R indices [I>2σ(I)]	R1=0.0470, wR2=0.1140
Peak and hole e. $Å^{-3}$	0.437 and −0.558
CCDC deposition no.	670,882

120 μM in concentration and increasing concentrations of complex (0 μM, 40 μM).

Viscosity experiments were carried on an Ubbelodhe viscometer, immersed in a thermostated water-bath maintained to 15.0°C, 25.0°C and 35.0°C. Titrations were performed for the Cu (II) complex (1–6 μM), and the complex was introduced into DNA solution (50 μM) present in the viscometer. Flow time was measured with a digital stopwatch and each sample was measured three times and an average flow time was calculated.

Cell culture and cytotoxicity assay

Cells were supplied by the School of Pharmacy, Lanzhou University (Lanzhou, China). Cells were routinely kept in RPMI-1640 medium supplemented with 10 % fetal bovine serum, penicillin G (100 U/mL) and streptomycin (100 μg/mL) at 37°C in a humidified atmosphere containing 5% CO_2. After a confluent cell layer was formed, the cells were harvested from the adherent cultures using 0.25 % trypsin + 0.02 % EDTA in phosphate buffered saline or D-Hank's buffer for 5 min. Suspensions were adjusted to cell densities of 5×10^4 cells/mL in order to ensure exponential growth throughout drug exposure. Aliquots of these suspensions were seeded into 96-well microcultures (90 μL / well). After incubation for 24 h, cells were exposed to the tested compounds of serial concentrations. The complex was dissolved in ethanol and diluted with RPMI-1640 to the required concentrations prior to use. After addition, the different concentration of complex (10 μL/well) and incubation for 68 h, 10 μL of aqueous MTT solution (5 mg/mL) was added to each well, and the cells were incubated continually for another 4 h. The medium and MTT mixtures were removed and the formazan crystals were dissolved in 100 μL DMSO/ cell. The absorbance of each cell at 570 nm was determined by analysis with a microplate spectrophotometer (EL_X800, U.S.A.), and the percentage cell viability was determined by dividing the average absorbance of each column of Cu (II)-treated wells by the average absorbance of the control wells. The growth inhibitory rate of treated cells was calculated by $(OD_{control} - OD_{test}) / OD_{control}\times100$ %. The IC_{50} values were determined by plotting the percentage viability versus concentration on a logarithmic graph and reading off the concentration at which 50 % of cells remain viable relative to the control. Each experiment was repeated at least three times to get the mean values.

Results and discussion

A polyether ring was chemically appended to the 1,8-dihydroxyxanthone structure to improve the hydrophilicity of the xanthone moiety and to further enhance the coordination to metal ions. Addition of 1 equiv of copper perchlorate salt to **L** in acetoneitrile yields the 1:1 metal-ligand Cu (II) complex, which is stable in atmospheric conditions and soluble in acetonitrile, acetone, ethanol, methanol, DMF and DMSO. The elemental analyses result indicates that Cu (II) ion is coordinated by two acetonitrile molecules, which has been confirmed by crystallography.

The characterization of complex

The structure of Cu (II) complex is depicted in Fig. 2. The Cu^{2+} cation is located inside the macrocycle of **L**, coordinated to four ligand oxygens, including the intra-annular carbonyl oxygen. Two acetonitrile molecules, above and below the plane of the macrocycle, are bound to the Cu^{2+} ion as well (Cu-N1=1.963 (2) Å and Cu-N2=1.963 (3) Å). The coordination number for the copper equals six. The Cu^{2+} metal center is not centered within the macrocyclic cavity in the structure, the cation is displaced toward O7 (Cu-O7=2.967Å, as opposed to Cu-O3=3.417Å), the geometry around copper is a distorted square bipyramid. The xanthone is virtually planar and the dihedral angle formed between the two aromatic ring planes of the xanthone is only 4.09° while in free ligand the dihedral angle is 14.49°, and the C=O bond length of C12-O2, 1.255Å is slightly longer than the free ligand 1.212Å [26]. The data indicate that, subsequent to Cu^{2+} coordination, the planarity of the xanthone ring increases thereby enhancing the DNA binding ability of the xanthone-Cu complex. Other important bond distances are listed in Table 2.

The ν (C=O) vibration of the free ligand is at 1,666.0 cm^{-1}, for Cu (II) complex, the peak shifts to 1,641.3 cm^{-1} and the $\Delta\nu_{(ligand\text{-}complex)}$ is 25 cm^{-1}. A weak band, which appears at 471.8 cm^{-1} after reaction with copper perchlorate salt, is assigned to ν (M-O). These date suggest that the oxygen of the carbonyl has formed a coordination bond with the Cu^{2+} cation. Moreover, the absorption band near 628.1 cm^{-1} indicates that free perchlorate is present [27]. The result of IR spectra was consistent with the X-ray crystallographic studies.

Solution chemistry and stability studies

As shown in Fig. 3, freshly prepared buffered solution of Cu (II) complex, two absorption bands are observed in the ultraviolet region, one at 243 nm and the other at 308 nm. No distinct shift changes or isobestic points in absorption spectra of complex can be observed in the following 72 h, and the color of the solution stays colorless and clear over 72 h monitored. It indicated that Cu (II) complex was stable and inert in aqueous solution.

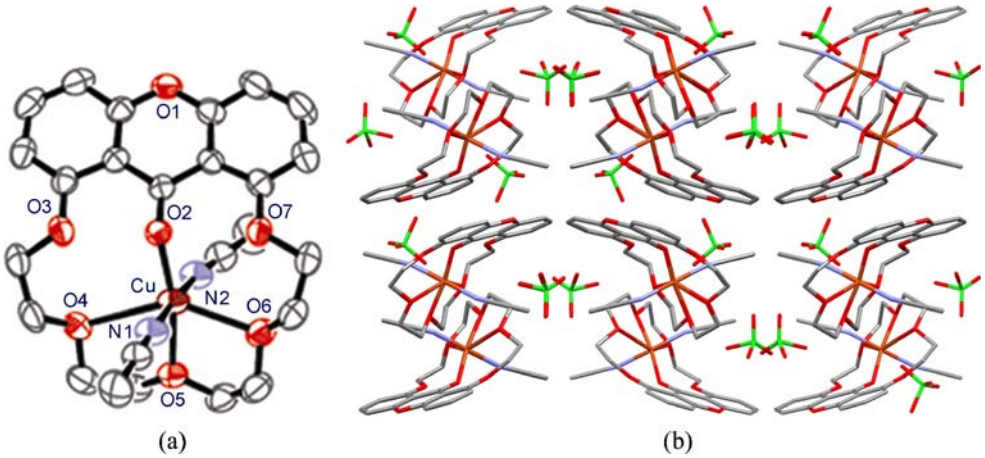

Fig. 2 **a** Thermal ellipsoid diagram of Cu (II) complex (Perchlorate anions and hydrogen atoms have been excluded for clarity. **b** The 2-D extended framework of Cu (II) complex

DNA-binding modes and affinities

In order to understand the mechanism of action of the Cu(II) complex, we decided to investigate the mode and affinity of its binding to DNA and to look for any correlation between the DNA binding in vivo and anticancer activity in vitro.

Electronic absorption spectra

The observation of hypochromism when an aromatic dye binds to double helical DNA is usually characteristic of intercalation between DNA base pairs by the dye, promoted by the strong stacking interaction between the aromatic chromophore and the base pairs [28]. As shown in Fig. 4, in the absence of DNA, the UV-Vis absorption spectra of Cu (II) complex has a strong π-π* transitions band at λ_{max}= 243 nm and a medium n-π* transitions band at λ_{max}= 308 nm. Upon addition of 1 equiv DNA, the absorption bands of Cu (II) complex at about 243 nm and 308 nm exhibit visible hypochromism of about 13.59% and 7.28%, respectively. The hypochromism observed for the bands of Cu (II) complex is accompanied by a small red shift by less than 4 nm. The above phenomena imply that the Cu (II) complex interacts with ct DNA probably by intercalating the xanthone ring into the base pairs.

From the absorption data, the binding constant K_b was determined using the Equation (1) [29], $[DNA]/(\varepsilon_a-\varepsilon_f)=[DNA]/(\varepsilon_b-\varepsilon_f)+1/K_b(\varepsilon_b-\varepsilon_f)$ (1), where [DNA] is the concentration of ct DNA in base pairs, ε_a, ε_f, and ε_b are the apparent extinction coefficient correspond to $A_{obsd}/[M]$, the extinction coefficient for the free compound and the extinction coefficient for the compound in the fully bound form, respectively. In plots of $[DNA]/(\varepsilon_a-\varepsilon_f)$ versus [DNA], K_b is given by the ratio of slope to the intercept (Fig. 4, inset). The binding constant K_b of the Cu (II) complex was $1.62\times10^4 M^{-1}$.

Furthermore, the observation of hyperchromic or hypochromic changes in the spectra due to the interaction of a small molecule with DNA is indicative of a conformational change in the DNA [30, 31]. Hyperchromism results from the damage of the DNA double helix structure, while hypochromism results from the contraction of DNA in the

Table 2 Selected bond lengths (Å)

$[Cu{\cdot}\mathbf{L}{\cdot}(CH_3CN)_2](ClO_4)_2$	
Cu-O2 (···O=C)	1.9166(19)
Cu-O4 (···O-CH_2)	2.690(2)
Cu-O5 (···O-CH_2)	2.0309(19)
Cu-O6 (···O-CH_2)	2.409(2)
Cu-N1 (···$NCCH_3$)	1.963(2)
Cu-N2 (···$NCCH_3$)	1.963(3)
C12-O2 (O=C)	1.255(3)
C22-N1 (C≡N)	1.119(3)
C24-N2 (C≡N)	1.123(4)

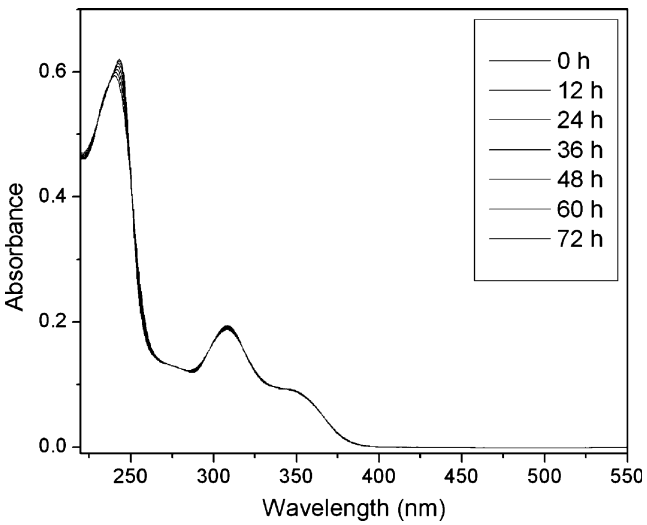

Fig. 3 Time-dependent UV-vis absorption spectra of Cu (II) complex in Tris-HCl buffer at 25°C recorded with time

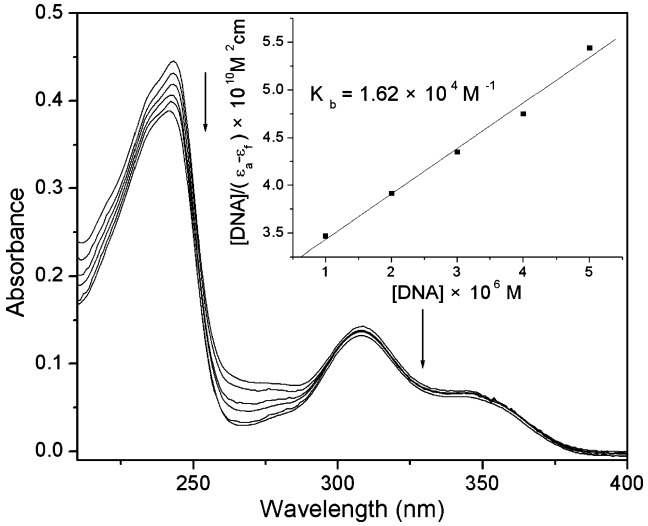

Fig. 4 UV-Vis absorption spectra of the Cu (II) complex upon addition of ct DNA. C_{Cu}=5 μM, C_{DNA}=0 μM, 1 μM, 2 μM, 3 μM, 4 μM, 5 μM. The inset is plot of [DNA]/(ε_b-ε_f) vs C_{DNA} for the titration of DNA to complex

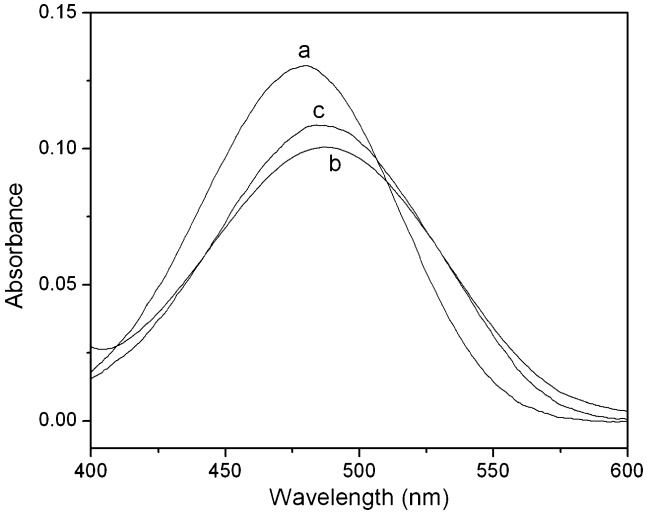

Fig. 6 The visible absorption spectra of 10 μM EB (**a**); 10 μM EB +10 μM DNA (**b**); 10 μM EB +10 μM DNA + 5 μM Cu (II) complex (**c**)

helix axis, as well as from the change in conformation on DNA. Figure 5 shows the absorption spectra of DNA alone in the presence of Cu (II) complex with various concentrations. The absorption increased significantly upon addition of complex, indicating interaction of the complex with DNA. This is a typical hyperchromic effect, which shows the damage of the DNA double helix structure after the Cu (II) complex bound to DNA.

In order to examine the binding mode of DNA with Cu (II) complex, ethidium bromide (EB) was employed in this experiment, as EB interacts presumably with DNA as a typical indicator of intercalation. Figure 6 shows that the maximal absorption of EB at 479 nm decreased and shifted to 487 nm in the presence of DNA, which is characteristic of intercalation. The curve C in Fig. 6 shows the absorption spectrum of a solution containing EB, Cu (II) complex and DNA. It was found that the absorption at 487 nm increased in comparison with that shown in curve B of Fig. 6.

It could result from two reasons: (1) EB bound to the Cu (II) complex strongly, resulting in the decrease of the amount of EB intercalated into DNA; (2) there exist competitive intercalation between the Cu (II) complex and EB with DNA, so releasing some free EB from DNA-EB complex [32]. However, the former reason could be precluded because no new absorption peak was seen.

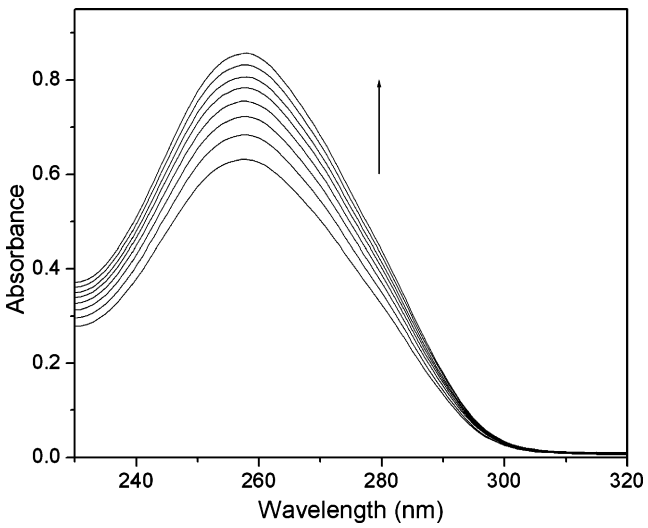

Fig. 5 UV-Vis absorption spectra of ct DNA upon addition of the Cu (II) complex. C_{DNA}=10 μM, C_{Cu}=0 μM, 1 μM, 1 μM, 2 μM, 3 μM, 4 μM, 5 μM, 6 μM, 7 μM

Fluorescence spectra

Concomitant with the hypochromism in absorption spectra of Cu (II) complex upon addition of ct DNA, an obvious fluorescent emission enhancement of the complex at 450 nm occurs as well. The fluorescent emission titration for the Cu (II) complex is illustrated in Fig. 7. The result suggests that the Cu (II) complex can be protected efficiently from solvent water molecules by the hydrophobic environment inside the DNA helix. This indicates that the complex can insert between DNA base pairs deeply, which is consistent with the above absorption spectral results. Since the hydrophobic environment inside the DNA helix reduces the accessibility of solvent water molecules to the complex and the complex mobility is restricted at the binding site, a decrease of the vibrational modes of relaxation results. The binding of the Cu (II) complex to DNA leads to a marked increase in emission intensity, which also agrees with those observed for other intercala-

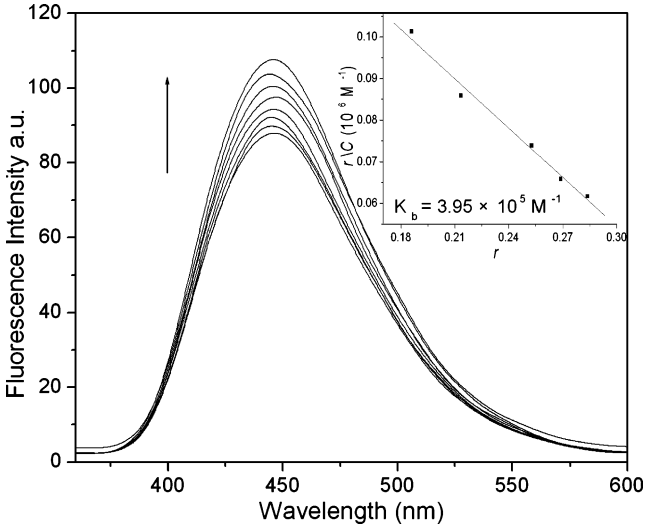

Fig. 7 Fluorescence emission spectra of the Cu (II) complex in the presence of increasing amounts of ct DNA. (λ_{ex}=320 nm, λ_{em}=350–600 nm) C_{Cu}=5 μM, C_{DNA}=0 μM, 2.5 μM, 5 μM, 7.5 μM, 10 μM, 12.5 μM, 15 μM, 17.5 μM. The inset is Scatchard plot of the fluorescence titration data of the complex

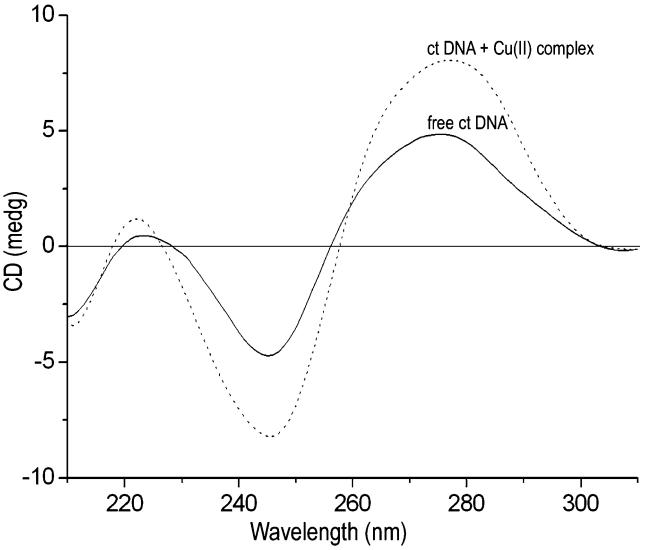

Fig. 9 CD Spectra of ct DNA (120 μM) in the in the absence and presence of the Cu (II) complex (40 μM)

tors [33]. According to the Scathchard equation (Fig. 7, inset), a plot of γ / C_f versus γ gave the binding constant $3.95\times10^5 M^{-1}$ from the fluorescence data for the complex, where γ is binding ratio C_b / $[DNA]_t$.

The concentration of the bound compound was calculated using Equation (2) [33], $C_b = C_t\ [(F-F_0)\ /\ (F_{max}-F_0)]$ (2), where C_t is the total compound concentration, F is the observed fluorescence emission intensity at given DNA concentration, F_0 is the intensity in the absence of DNA and F_{max} is the fluorescence of the totally bound complex. The concentration of the free compound C_f is equal to C_t–C_b.

Further support for Cu (II) complex binding to DNA by intercalation mode is given through the competitive binding experiment. Figure 8 shows the emission spectra of DNA-EB system upon the increasing amounts of Cu (II) complex. It is well established that EB is useful as a DNA structure probe [34]. The emission intensity of DNA-EB system at 587 nm decreased as the concentration of the Cu (II) complex increased, which indicated that the complex could displace EB from the DNA-EB system. The result was due to the translocation of EB from a hydrophobic environment to an aqueous environment [15]. Such a characteristic change is often observed in intercalative DNA interactions [35].

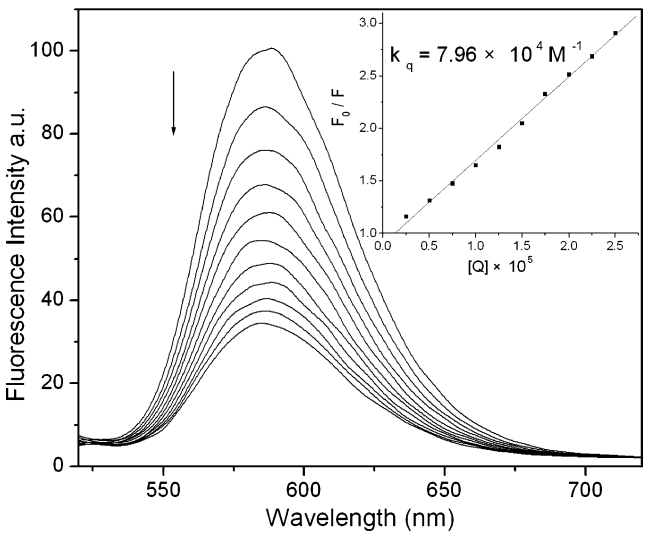

Fig. 8 Fluorescence emission spectra of DNA-EB in the absence and presence of increasing amounts of the Cu (II) complex. (λ_{ex}=500 nm, λ_{em}=520–720 nm) C_{EB}=2 μM, C_{DNA}=30 μM, C_{Cu}=0 μM, 2.5 μM, 5 μM, 7.5 μM, 10 μM, 12.5 μM, 15 μM, 17.5 μM, 20 μM, 22.5 μM, 25 μM. The inset is Stern-Volmer quenching plots

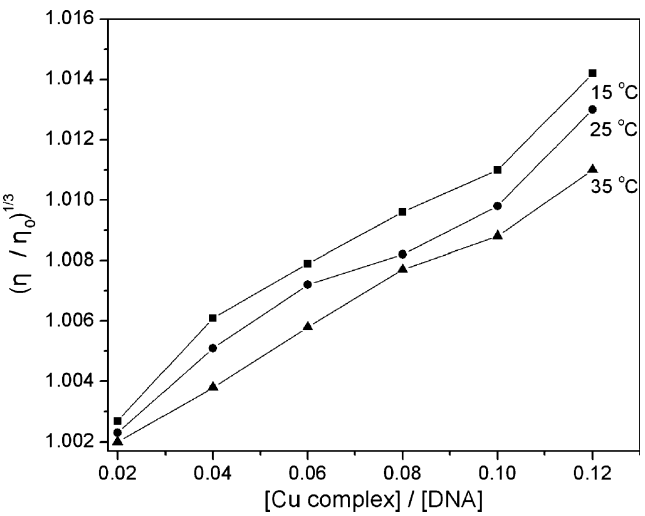

Fig. 10 Effect of increasing amounts of the Cu (II) xxcomplex on the relative viscosity of ct DNA at different temperatures. C_{DNA}=50 μM, C_{Cu}=1 μM, 2 μM, 3 μM, 4 μM, 5 μM, 6 μM

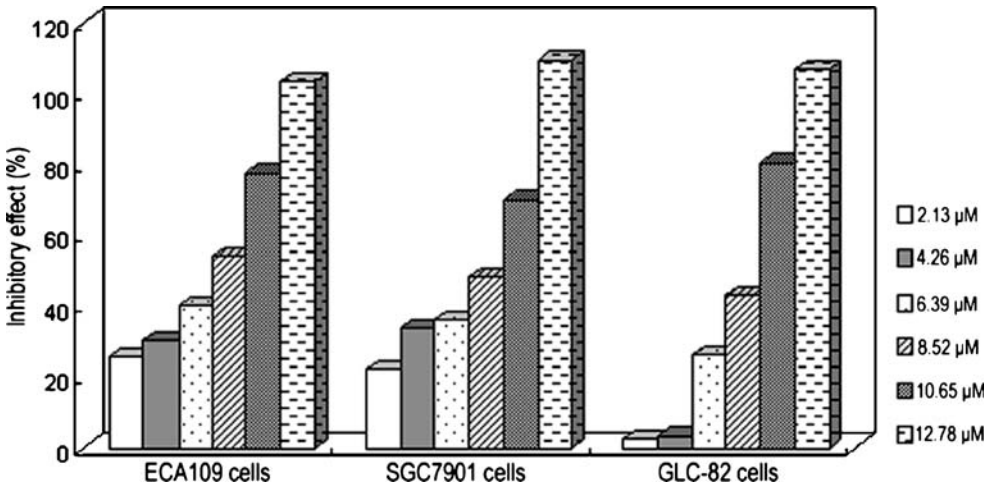

Fig. 11 Cytotoxicities of Cu (II) complex against various human cancer cells

According to the classical Stern-Volmer Equation (3) [36]: $F_0/F=1+K_q[Q]$ (3), where F_0 and F represent the emission intensity in the absence and presence of quencher, respectively, K_q is a linear Stem-Volmer quenching constant and [Q] is the quencher concentration. The quenching plots illustrate that the quenching of EB bound to DNA by the complex is in good agreement with the linear Stern-Volmer equation (Fig. 8, inset). In the plots of F_0/F versus [Q], K_q is given by the ratio of the slope to the intercept. The K_q value for complex is $7.96\times10^4 M^{-1}$. As these changes indicate only one quenching process, it may be concluded that the complex binds to DNA solely by intercalation mode.

Circular dichroic spectra

Circular dichroic spectral techniques give us useful information on how the conformation of DNA is influenced by the binding of small molecules. The CD spectrum of ct DNA consists of a positive band at 275 nm due to base stacking and a negative band at 245 nm due to helicity, which is characteristic of DNA in the right-handed B form [37]. The changes in CD signals of DNA observed on interaction with small molecules may often be assigned to the corresponding changes in DNA structure [38]. Thus simple groove binding and electrostatic interaction of small molecules show less or no perturbation on the base-stacking and helicity bands, whereas intercalation enhances the intensities of both the bands stabilizing the right-handed B conformation of DNA as observed for the classical intercalator methylene blue [39]. The CD spectra of DNA taken after incubation of the complex with ct DNA are shown in Fig. 9. The intensities of both the negative and positive bands increase significantly, which are typical of strong intercalation involving π-stacking and stabilization of the right-handed B form of ct DNA. Thus the CD spectral results are consistent with the intercalative mode of DNA binding for the present complexes. It is possible that the extended aromatic rings reduce the helical twist angle of the DNA base pairs and increase the intensity of the base stacking band [39].

Viscosity measurements

Optical photophysical probes generally provide necessary, but not sufficient, clues to support a binding model. Hydrodynamic measurements that are sensitive to length change (i.e. viscosity and sedimentation) are regarded as the least ambiguous and the most critical tests of binding model of small molecule to DNA in solution in the absence of crystallographic structural data. A classical intercalation model results in lengthening the DNA helix as base pairs are separated to accommodate the binding small molecules, leading to the increase of DNA viscosity. In contrast, a partial and non-classical intercalation of small molecules could bend or kink the DNA helix, reduce its effective length and, concomitantly, its viscosity [40, 41].

To confirm the above results, viscosity measurements were carried out and the results are presented as $(\eta / \eta_0)^{1/3}$ versus binding ratio, where η is the viscosity of DNA in the presence of complex, and η_0 is the viscosity of DNA alone. Viscosity values were calculated from the observed flow time of DNA-containing solution corrected from the flow time of butter alone (t_0), $\eta = t\text{-}t_0$ [42, 43].The results demonstrate that the Cu (II) complex can intercalate between adjacent DNA base pairs, causing an extension in the helix, and thus increase the viscosity of DNA (Fig. 10). Moreover, the change of viscosity decreased slightly when

Table 3 The IC_{50} values of Cu (II) complex against various human cancer cells

Cell	ECA109 (esophagus)	SGC7901 (stomach)	GLC-82 (lung)
IC_{50}(μM)	14.24	17.73	17.86

the temperature was increased from 15.0°C to 35.0°C. It demonstrated that the viscosity decrease occurred as a result of decreased stability of the complex, and thus lowered the binding affinity to DNA.

In vitro antitumor potency

Cytotoxicity tests were performed using the MTT assay, following exposure of three human cancer cell lines, ECA109 (esophagus squamous cancer), SGC7901 (stomach cancer) and GLC-82 (lung cancer) in vitro to the synthesized complex at increasing concentrations for 72 h. The cytotoxicities of complex is obvious (Fig. 11), and the IC_{50} values are less-than 18 μM in three of cells (Table 3). It can be inferred that the Cu (II) complex exhibit very effective anticancer activity.

Conclusion

A novel Cu (II) complex of $[Cu{\cdot}\mathbf{L}{\cdot}(CH_3CN)_2](ClO_4)_2$ has been synthesized and characterized. The DNA binding properties have been investigated by spectrophotometric methods and viscosity measurements, the cytotoxicity assay of complex has been tested by MTT method. The results support the fact that the xanthone ring changes to be more planar and more conjugated after the Cu (II) complex formed and the complex can intercalate into the DNA base pair because of the good planarity of the xanthone ring. The result of inhibitory effect in vitro is consistent with the result of DNA binding study. We conclude that the new xanthone-Cu complex intercalates between DNA base pairs and causes DNA damage in cancer cells, thus inhibiting the division of cancer cells. Information obtained from the present work provides evidence for the nature of the binding of the xanthone-Cu complex to DNA and is expected to offer further impetus for designing newer probes for DNA structure and novel therapeutic agents that are directed at DNA.

Acknowledgement We are grateful to the School of Pharmacy, Lanzhou University for their support.

References

1. Liu CL, Wang M, Zhang T, Sun HZ (2004) DNA hydrolysis promoted by di- and multi-nuclear metal complexes. Coord Chem Rev 248:147–168. doi:10.1016/j.cct.2003.11.002
2. Metcalfe C, Thomas JA (2003) Kinetically inert transition metal complexes that reversibly bind to DNA. Chem Soc Rev 32:215–224. doi:10.1039/b201945k
3. Keenea FR, Smitha JA, Collins, JG (2009) Metal complexes as structure-selective binding agents for nucleic acids. Coord Chem Rev (in press). doi:10.1016/j.ccr.2009.01.004
4. Erkkila KE, Odom DT, Barton JK (1999) Recognition and reaction of metallointercalators with DNA. Chem Rev 99:2777–2796. doi:10.1021/cr9804341
5. Jiang Q, Xiao N, Shi PF, Zhua YG, Guo ZJ (2007) Design of artificial metallonucleases with oxidative mechanism. Coord Chem Rev 251:1951–1972. doi:10.1016/j.ccr.2007.02.013
6. Yang P, Guo ML (1999) Interactions of organometallic anticancer agents with nucleotides and DNA. Coord Chem Rev 185–186:189–211. doi:10.1016/S0010-8545(98)00268-9
7. Carter MT, Rodriguez M, Bard AJ (1989) Voltammetric studies of the interaction of metal chelates with DNA. 2. Tris-chelated complexes of cobalt(III) and iron(II) with 1,10-phenanthroline and 2,2′-bipyridine. J Am Chem Soc 111:8901–8911. doi:10.1021/ja00206a020
8. Reddy PR, Rao KS, Satyanarayana B (2006) Synthesis and DNA cleavage properties of ternary Cu(II) complexes containing histamine and amino acids. Tetrahedron Lett 47:7311–7315. doi:10.1016/j.tetlet.2006.08.033
9. Kumar RS, Arunachalam S, Periasamy VS, Preethy CP, Riyasdeen A, Akbarsha MA (2009) Surfactant–cobalt(III) complexes: Synthesis, critical micelle concentration (CMC) determination, DNA binding, antimicrobial and cytotoxicity studies. J Inorg Biochem 103:117–127. doi:10.1016/j.jinorgbio.2008.09.010
10. Ji LN, Zhou XH, Liu JG (2001) Shape- and enantioselective interaction of Ru(II)/Co(III) polypyridyl complexes with DNA. Coord Chem Rev 216:513–536. doi:10.1016/S0010-8545(01)00338-1
11. Li YP, Wu YB, Zhao J, Yang PJ (2007) DNA-binding and cleavage studies of novel binuclear copper(II) complex with 1, 1′-dimethyl-2, 2′-biimidazole ligand. Inorg Biochem 101:283–290. doi:10.1016/j.jinorgbio.2006.10.004
12. Zuber G Jr, Quada JC, Hecht SM (1998) Sequence Selective Cleavage of a DNA Octanucleotide by Chlorinated Bithiazoles and Bleomycins. J Am Chem Soc 120:9368–9369. doi:10.1021/ja981937r
13. Li VS, Choi D, Wang Z, Jimenez LS, Tang MS, Kohn H (1996) Role of the C-10 Substituent in Mitomycin C-1-DNA Bonding. J Am Chem Soc 118:2326–2331. doi:10.1021/ja953871v
14. Zhang H, Liu CS, Bu XH, Yang M (2005) Synthesis, crystal structure, cytotoxic activity and DNA-binding properties of the copper (II) and zinc (II) complexes with 1-[3-(2-pyridyl)pyrazol-1-ylmethyl]naphthalene. J Inorg Biochem 99:1119–1125. doi:10.1016/j.jinorgbio.2005.02.005
15. Zeng YB, Yang N, Liu WS, Tang N (2003) Synthesis, characterization and DNA-binding properties of La(III) complex of chrysin. J Inorg Biochem 97:258–264. doi:10.1016/S0162-0134(03)00313-1
16. Wang BD, Yang ZY, Wang Q, Cai TK, Crewdson P (2006) Synthesis, characterization, cytotoxic activities, and DNA-binding properties of the La(III) complex with Naringenin Schiff-base. Bioorg Med Chem 14:1880–1888. doi:10.1016/j.bmc.2005.10.031
17. Zhou J, Wang LF, Wang JY, Tang N (2001) Synthesis, characterization, antioxidative and antitumor activities of solid quercetin rare earth(III) complexes. J Inorg Biochem 83:41–48. doi:10.1016/S0162-0134(00)00128-8
18. Nakatani K, Nakahata N, Arakawa T, Yasuda H, Ohizumi Y (2002) Inhibition of cyclooxygenase and prostaglandin E_2 synthesis by γ-mangostin, a xanthone derivative in mangosteen, in C6 rat glioma cells. Biochem Pharmacol 63:73–79. doi:10.1016/S0006-2952(01)00810-3
19. Wang LW, Kang JJ, Chen IJ, Teng CM, Lin CN (2002) Antihypertensive and vasorelaxing activities of synthetic xanthone derivatives. Bioorg Med Chem 10:567–572. doi:10.1016/S0968-0896(01)00315-7
20. Liu Y, Ma L, Chen WH, Wang B, Xu ZL (2007) Synthesis of xanthone derivatives with extended π-systems as α-glucosidase inhibitors: Insight into the probable binding mode. Bioorg Med Chem 15:2810–2814. doi:10.1016/j.bmc.2007.02.030

21. Jackson WT, Boyd RJ, Froelich LL, Gapinski DM, Mallett BE, Sawyer JS (1993) Design, synthesis, and pharmacological evaluation of potent xanthone dicarboxylic acid leukotriene B_4 receptor antagonists. J Med Chem 36:1726–1734. doi:10.1021/jm00064a006
22. Mills OS, Mooney NJ, Robinson PM, Watt CF, Box BG (1995) Preparation and properties of some crown ethers incorporating stable carbocations. J Chem Soc Perkin Trans 2 697–706. doi:10.1039/p29950000697
23. CSJ (ed) (1986) Synthetical handbook for inorganic compounds II. Chemical Industry, Beijing
24. Michael TC, Marisol R, Allen JB (1989) Voltammetric studies of the interaction of metal chelates with DNA. 2. tris-chelated complexes of cobalt(III) and iron(II) with 1,10-phenanthroline and 2,2′-bipyridine. J Am Chem Soc 111:8901–8911. doi:10.1021/ja00206a020
25. Kumar CV, Asuncion EH (1993) DNA binding studies and site selective fluorescence sensitization of an anthryl probe. J Am Chem Soc 115:8547–8553. doi:10.1021/ja00072a004
26. Beddoes RS, Cox BG, Mills OS, Mooney NJ, Watt CF, Kirkland D, Martin D (1996) Structures and complexing properties of crown ethers incorporating 1,8-dioxyxanthones. J Chem Soc Perkin Trans 2 2091–2098. doi:10.1039/p29960002091
27. Nakamato K (1978) Infrared and raman spectra of inorganic and coordination compound, 3rd edn. Wiley-Interscience, New York
28. Bloomfield VA, Crothers DM, Tinoco I Jr (1974) Phsical chemistry of nucleic acids. Harper & Row, New York
29. Wolf A, Shimer GH Jr, Meehan T (1987) Polycyclic aromatic hydrocarbons physically intercalate into duplex regions of denatured DNA. Biochemistry 26:6392–6396. doi:10.1021/bi00394a013
30. Zhou CY, Zhao J, Wu YB, Yin CX, Yang P (2007) Synthesis, characterization and studies on DNA-binding of a new Cu(II) complex with N1, N8-bis(l-methyl-4-nitropyrrole-2-carbonyl)triethylenetetramine. J Inorg Biochem 101:10–18. doi:10.1016/j.jinorgbio.2006.07.011
31. Zhou QH, Yang P (2006) Crystal structure and DNA-binding studies of a new Cu(II) complex involving benzimidazole. Inorg Chim Acta 359:1200–1206. doi:10.1016/j.ica.2005.11.003
32. Boger DL, Fink BE, Brunette SR, Tse WC, Hedrick MP (2001) A Simple, high-resolution method for establishing DNA binding affinity and sequence selectivity. J Am Chem Soc 123:5878–5891. doi:10.1021/ja010041a
33. Satyanarayana S, Dabrowiak JC, Chaires JB (1992) Neither Δ- nor Λ-tris(phenanthroline)ruthenium(II) binds to DNA by classical intercalation. Biochemistry 31:9319–9324. doi:10.1021/bi00154a001
34. Lippard SJ (1978) Platinum complexes: probes of polynucleotide structure and antitumor drugs. Acc Chem Res 11:211–217. doi:10.1021/ar50125a006
35. Kumar CV, Barton JK, Turro NJ (1985) Photophysics of ruthenium complexes bound to double helical DNA. J Am Chem Soc 107:5518–5523. doi:10.1021/ja00305a032
36. Eftink MR, Ghiron CA (1981) Fluorescence quenching studies with proteins. Anal Biochem 114:199–227. doi:10.1016/0003-2697(81)90474-7
37. Ivanov VI, Minchenkova LE, Schyolkina AK, Poletayev AI (1973) Different conformations of double-stranded nucleic acid in solution as revealed by circular dichroism. Biopolymers 12:89–110. doi:10.1002/bip. 1973.360120109
38. Lincoln P, Tuite E, Nordén B (1997) Short-Circuiting the Molecular Wire: Cooperative Binding of Δ-[Ru(phen)2d ppz]2+ and Δ-[Rh(phi)2bipy]3+ to DNA. J Am Chem Soc 119:1454–1455. doi:10.1021/ja9631965
39. Nordén B, Tjerneld F (1982) Structure of methylene blue-DNA complexes studied by linear and circular dichroism spectroscopy. Biopolymers 21:1713–1734. doi:10.1002/bip. 360210904
40. Zou XH, Ye BH, Li H, Liu JG, Xiong Y, Ji LN (1999) Mono- and bi-nuclear ruthenium(II) complexes containing a new asymmetric ligand 3-(pyrazin-2-yl)-as-triazino [5,6-f]1,10-phenanthroline: synthesis, characterization and DNA-binding properties. J Chem Soc Dalton Trans 1423–1428. doi:10.1039/a900064j
41. Sigman DS, Mazumder A, Perrin DM (1993) Chemical nucleases. Chem Rev 93:2295–2316. doi:10.1021/cr00022a011
42. Eriksson M, Leijon M, Hiort C, Norden B, Gradslund A (1994) Binding of Δ- and Λ-$[Ru(phen)_3]^{2+}$ to $[d(CGCGATCGCG)]_2$ Studied by NMR. Biochemistry 33:5031–5040. doi:10.1021/bi00183a005
43. Xiong Y, He XF, Zou XH, Wu JZ, Chen XM, Ji LN, Li RH, Zhou JY, Yu KB (1999) Interaction of polypyridyl ruthenium(II) complexes containing non-planar ligands with DNA. J Chem Soc Dalton Trans 19–23. doi:10.1039/a806170j